

N78-14586 256

USE OF AN INERTIAL NAVIGATION SYSTEM FOR ACCURATE TRACK RECOVERY  
AND COASTAL OCEANOGRAPHIC MEASUREMENTS

B.M. Oliver and J.F.R. Gower

Institute of Ocean Sciences  
Department of Fisheries and Environment  
Victoria, B.C., Canada V8W 1Y4

ABSTRACT

A data acquisition system using a Litton LTN-51 inertial navigation unit (INU) has been tested and used for aircraft track recovery and for location and tracking from the air of targets at sea. The characteristic position drift of the INU is compensated for by sighting landmarks of accurately known position at discrete time intervals using a visual sighting system in the transparent nose of the Beechcraft 18 aircraft used. The angular direction data from the sight in conjunction with the aircraft's attitude and barometric altitude, enables the aircraft's 'true' position to be determined. A modified cubic spline interpolation routine was then used to approximate the continuous drift of the INU with time. For an aircraft altitude of about 300 m, theoretical and experimental tests indicate that calculated aircraft and/or target positions obtained from the interpolated INU drift curve will be accurate to within 10 m for landmarks spaced approximately every 15 minutes in time.

For applications in coastal oceanography, such as surface current mapping by tracking artificial targets, the system allows a broad area to be covered without use of high altitude photography and its attendant needs for large targets and clear weather. Data is collected in digital form enabling the data to be easily processed and the results plotted directly.

---

1. INTRODUCTION

For many airborne remote sensing applications, an accurate record of aircraft position is essential. Over land, a simple and widely used technique for obtaining this information is to compare photographs taken during the flight with accurate control maps of the flight path area. This technique is awkward, time consuming and cannot in general be used over water unless the area to be studied is sufficiently close to the shore or to known navigation markers. Several radar based or low frequency radio systems are also available, but these are either not very precise (errors of  $\approx 100$  m) or require the setting up of auxiliary ground stations.

Inertial navigation produces an extremely precise measurement of aircraft position and attitude, but has associated with it a reasonably large drift error in position which, if uncorrected, would prove to be unacceptable for many remote sensing applications. This characteristic drift can be compensated for in hybrid systems in which data from a less precise but drift free sensor

Preceding page blank

are also used<sup>1,2</sup>. The system described here uses a visual sight to make periodic fixes on landmarks of known position to correct the drift error, resulting in track recovery accurate to  $\pm 10$  meters. This system has been investigated for use in flight path recovery for airborne survey operations<sup>3</sup>. A particular advantage of using a sighting system for establishing aircraft fixes is that the same apparatus may also be used to determine the positions of additional sighted targets such as floating drogues or linear surface features.

This paper describes the system configuration and the computations by which the INS drift errors are determined from the sighting data. Results of tests of system accuracy are presented, and several oceanographic applications in mapping sea surface features and currents are discussed in detail.

## 2. INERTIAL SYSTEM AND TARGET SIGHTING APPARATUS

Details of the inertial/sighting system have been described previously,<sup>3</sup> therefore, only a brief description is presented here. The inertial navigation unit used was a Litton LTN-51 with standard software designed for airline navigation. The unit operates by sensing aircraft accelerations along three mutually perpendicular axes on a gyrostabilized level platform. The platform is maintained level by applying torquing signals to the gyro axes derived from the movement of the aircraft over the earth's surface. The computations necessary to provide the correct torquing signals are performed by the unit's own internal digital computer. These calculations assume a spheroidal earth with a flattening ratio of 1:297 and a constant aircraft altitude of about 10,000 m. This computer also calculates standard output data from the INU including aircraft position and velocity data as well as navigation information useful in commercial airline operations. In addition, high accuracy aircraft attitude (pitch, roll and azimuth) is available directly from angle resolvers attached to the level platform.

The standard output data is of limited value, however, because of two factors; 1) the computer cycle time gives relatively infrequent updating of this data and 2) intentional internal rounding reduces its accuracy. In order to circumvent these problems, a specialized data acquisition system, MIDAS (Marine Inertial Data Acquisition System), was developed. MIDAS was designed and constructed by MacDonald Dettwiler and Associates Ltd. of Vancouver and is an outgrowth of the system they designed and constructed for the Canada Centre for Remote Sensing in Ottawa<sup>4</sup>. MIDAS allows direct readout of the INU's internal computer memory, so as to give rapid access to the high precision navigation data. This data is output at a rate of 20 samples/sec and is used to calculate high precision aircraft position, velocity and direction. MIDAS allows, in addition, data input from eight analog channels (100 samples/sec) as well as other user supplied sensors. This data together with the observation time is subsequently output to either video or industry compatible magnetic tape. In the latter case, the user has the option of choosing between several recording modes depending on the frequency at which data recording is desired.

The target sighting apparatus consists of a zero parallax shotgun sight on an alt/azimuth mount located in the transparent nose of the aircraft, a Beechcraft 18. A precision potentiometer on each axis of the mount enables the sighting angles relative to the aircraft to be monitored. This is accomplished by placing a regulated dc voltage across each potentiometer resulting in an output dc voltage proportional to the sighting angles. The output voltages from these potentiometers are input to two of the analog channels. Operation of the sight is controlled by an observer lying in the nose of the aircraft. During the flight, the observer aims the sight at either landmarks of known position or visible surface objects or features to be positioned. When the sight and the target are aligned, the operator pushes a 'record' button which places a positive voltage on a third analog channel, identifying the target for later processing. The magnitude of this voltage is controlled by the operator

and allows for up to 100 different targets to be identified.

As was mentioned previously, MIDAS allows several modes of recording data on magnetic tape. Normally, INS data is output at the maximum rate of 20 samples/sec (100 samples/sec for the analog channels). For most of the flights, however, where no additional sensors were present, INS and sight data needed only to be recorded at discrete time (i.e., when a target was being sighted) and in short bursts lasting about one second. In order to reduce the amount of output data in these flights, MIDAS was modified to allow for a much slower background recording rate of only one sample/sec. In this mode, continuous recording is re-enabled while the 'record' button is pressed. The one sample/sec background recording rate was found to be more than adequate for post flight track recovery.

Calibration of the sight in the laboratory resulted in an estimated RMS error of  $0.18^\circ$ . Additional calibrations of the sight in the aircraft were also performed in order to establish the orientation of the sight mount with respect to the INU. It is estimated that the combined calibration error is less than  $0.5^\circ$ .

### 3. INTERPOLATION OF INERTIAL SYSTEM DRIFT

In order to maintain the gyro-stabilized platform level as the aircraft moves over the earth's surface, the INU's internal computer provides gyro torquing voltages calculated from the measured horizontal movement of the aircraft. The LTN-51 inertial unit used in this study is 'Schuler tuned', that is, the torquing voltages are made proportional to the aircraft's angular velocity relative to the center of the earth. The inertial platform, therefore, behaves as a Schuler pendulum<sup>1</sup> and as such, if perturbed undergoes stable oscillation about the level position with a period T given by

$$T = 2\pi\left(\frac{R}{g}\right)^{\frac{1}{2}} \quad (1)$$

where R is the earth's radius and g is the acceleration of gravity. This oscillation, which has a period T = 84.4 minutes, results in an approximately sinusoidal drift in the calculated positions (latitude and longitude) returned by the INU. The fact that the INU drift is not perfectly sinusoidal arises from additional error mechanisms within the inertial system. The amplitude of the mean drift, in normal circumstances, is of the order of 2 km per hour.

Utilizing the target sighting apparatus, the magnitude of this drift may be determined at discrete times by sighting landmarks on the earth's surface of accurately known position. The angular direction data from the sight in conjunction with the aircraft's attitude and barometric altitude is used to establish the aircraft's 'true' position using the known position of the sighted landmark. It should be mentioned here, that the relatively large position drift of the INU results from only relatively small ( $\sim 1'$  arc) angular errors in the gyro-stabilized level platform. Thus errors present in the attitude data will be negligible in comparison to the estimated errors in the sighting angles. The difference between this 'true' position and that returned by the INU determine the error due to inertial system drift (north and east) at the time the target was sighted. During flight, target sightings were generally restricted to observing angles less than  $30^\circ$  off nadir in order to reduce the effects of errors in sighting angles and in the aircraft's indicated barometric altitude. For the present experimental system, it is estimated that for an aircraft altitude of 300 m these errors will be of the order of  $\pm 5$  m.

An estimate of the INU drift for intermediate times is then obtained by fitting a modified cubic spline to the resulting discrete drift data. A cubic spline was chosen over more complicated fitting procedures (e.g., Kalman Filtering)<sup>2,6</sup> on the grounds of simplicity and much reduced analysis time. It

should be noted, however, that a cubic spline interpolation will maintain a smoothly varying position and velocity drift and to this extent will tend to duplicate the actual drift behavior of the inertial system. In addition, a spline interpolation does not require continuous monitoring and/or recording of aircraft navigation and attitude data, a significant advantage for longer flights.

In order to estimate the possible errors involved in fitting a cubic spline to the discrete drift data, a theoretical study was carried out in which a modified cubic spline was fitted to a set of hypothetical drift measurements. The particular spline fitting routine used here differed from the classical spline fit in that the fitted curve was allowed to deviate from the data points by specifying an allowable maximum sum of squares error in the fitting routine. This procedure is more suited to the experimental conditions considered here where finite errors in individual position fixes are to be expected.

Postulating a sinusoidal velocity drift in the inertial system, the position and velocity drift, to first order, may be specified by the following equations;

$$v = A \cos(\omega t + \phi) + B \quad (2)$$

$$S = \frac{A}{\omega} \sin(\omega t + \phi) + Bt + C \quad (3)$$

where  $\omega = \frac{2\pi}{T}$ ,  $T = 84.4$  min and  $\phi$  is the phase angle. Comparing Eq. 3 with actual drift data obtained from test flights of the system indicates that for time periods up to several hours after initial inertial system alignment, the position drift is predominately sinusoidal ( $B \approx 0$ ) with  $A$  ranging between 1 and 2 m/sec. The value of  $C$ , although in general non-zero, is arbitrary for this study in that it has no effect on the fitting procedure.

The test procedure involved fitting a modified cubic spline to simulated drift curve data obtained from Eq. 3 for values of  $A$  between 1 and 5 m/s and fixed time intervals between data points of from 1 to 20 minutes. In order to allow for different starting phase angles,  $\phi$  was varied, for each time interval, from 0 to  $2\pi$  in steps of  $\pi/10$ . In addition, to further simulate actual experimental data, normally distributed random errors with a specified standard deviation  $\sigma$  were added to the individual data points. The maximum sum of squares error for the cubic spline routine was set so as to equate the RMS error in the data and the allowable RMS error in the spline fit. The RMS difference between the sinusoidal curves and the cubic spline was then computed for each case.

The results of these tests are shown in Figs. 1a and b. Here the effect on the RMS difference of varying  $\sigma$  with a fixed  $A$  and the effect of varying  $A$  with a fixed  $\sigma$  are plotted. The most striking feature in both plots is that for time intervals between data points ranging from 5 to 10 minutes (300-600 secs) the RMS difference, which represents the interpolation error in fitting the modified cubic spline to the sine curve, is essentially constant at a value equal to the assumed RMS error in the simulated data. Thus, for position fixes obtained every 5 to 10 minutes, the interpolation error in predicting the actual INU drift will be approximately determined by the accuracy to which the position fixes are obtained. For time intervals exceeding 10 minutes the interpolation error tends to increase fairly rapidly depending on the drift amplitude  $A$ . Conversely, for decreasing time intervals less than 5 minutes, the interpolation error approaches zero as errors in the many sightings tend to average out.

As was mentioned previously, a reasonable estimate for the RMS error in the positions fixes for the target sighting apparatus used here is  $\pm 5$  m.

Figure 1b, therefore, shows that for a typical value of  $A = 1.5$  m/sec, the RMS interpolation error will be less than 10 m if position fixes are obtained at least every 15 minutes. For the aircraft used in this study, this represents a ground distance of about 75 km.

It should be mentioned, however, that these error estimates will hold only if the drift of the inertial system behaves 'smoothly' between position fixes. This has been found to be largely the case for test flights of the present system. Maneuver dependent error mechanisms in the INU such as azimuth drift will introduce however, small errors in the indicated positions which will be largely a function of distance travelled from the nearest position fix and as such will not follow the time dependent Schuler drift. Azimuth errors of up to 50" arc have been identified in the present system in several test flights resulting in cross-track errors of up to 2.5 m per km. It is therefore evident that not only the time spacing of position fixes is important, but also the location of the study area relative to the reference landmarks. Specifically, for example, if the study area lies approximately along a line between two landmarks, the resulting ground position errors due to errors in azimuth will be minimized. For the test flights discussed here, the landmarks were chosen with this criterion in mind. It should be mentioned also that one advantage in Kalman Filter analysis is that errors of this type would be modelled as part of the total system error response and are therefore taken into account.

#### 4. FLIGHT TEST OF INERTIAL/SIGHTING SYSTEM

In order to determine the errors involved in using the inertial/sighting system for flight path recovery under actual in-flight conditions, several test flights were conducted both over land and over local coastal waters near Victoria. One such test flight was carried out along a relatively straight 30 km section of highway for which accurate 25,000 scale topographic maps were available. The flight path ran along the Patricia Bay Highway on Vancouver Island between Swartz Bay and the southern tip of the City of Victoria. The highway was flown in both directions (North/South) at an aircraft altitude of about 300 m. The purpose of the flight was to compare the calculated and measured positions of major road intersections at approximately 2 km intervals along the highway. Target positions and elevations above sea level were obtained from four separate topographic maps of the region. The target elevations were needed to compute the altitude of the plane over each sighted target. The actual position of each road intersection were obtained from the appropriate map of the area using a flat bed digitizer. Deviations between the known and calculated positions of each intersection are shown in Fig. 2. As is evident, the drift of the inertial system is relatively constant in latitude at about 560 m North, and in longitude varies from a minimum of 420 m to a maximum of 720 m East. A drift curve for the INS was calculated by fitting the modified cubic spline ( $\sigma = 5$  m) to the data from two of the road intersections located near the northern and southern ends of the highway and reference landmarks at the beginning and end of the overall flight path. The particular road intersections were chosen in order to obtain an approximately equal time spacing ( $\approx 6$  minutes) between the reference data. By interpolating along the cubic spline, the positions of the remaining road intersections were calculated and subsequently compared with their measured values. The resulting average errors in latitude and longitude were  $-5 \pm 9$  m and  $-7 \pm 9$  m respectively. These averages do not include data from the six most southerly intersections (see Fig. 2) because of a visible discontinuity across the boundary of the topographic map of that particular portion of the highway and the next adjoining map in the series. When averaged separately the data for these intersections showed an average error of  $23 \pm 6$  m in latitude and  $-14 \pm 7$  m in longitude. Considering that a significant portion of the above errors can be attributed to map and digitizer inaccuracies which could be as large as 10 m, these standard deviations compare favorably with the theoretical study described previously. Finally, Fig. 3 shows a map of the aircraft flight path corrected for INS drift using the fitted cubic spline. For comparison, the uncorrected flight path returned by the inertial system is also shown.

## 5. OCEANOGRAPHIC APPLICATIONS

As was discussed previously, one of the advantages in using a target sighting system for establishing inertial system drift is that the same sighting system may also be used to determine the position of secondary targets and/or surface features on the earth. This has particular application in the area of coastal oceanographic remote sensing; specifically, the monitoring of surface water movement in a variety of situations. Generally, these types of measurements are conducted by monitoring the movement of fluorescent dyes and/or floating drogues. These are monitored either by aerial photography<sup>7</sup> or, for the latter, by various electronic positioning systems<sup>8,9</sup>. In the studies referenced above, typical accuracies for position determination ranged from 100 to 200 m. This accuracy is sufficient for studies of gross surface motion, or which are to be conducted over a relatively long time span (1-2 hrs between sightings). For studies where the movement is restricted to a short period of time or where monitoring time is limited, however, this type of accuracy would likely be insufficient. In addition to this, aerial photography, which is heavily relied upon in dye dispersal or river outflow studies for example, is severely limited in some areas due to extended periods of low cloud cover. Cloud cover is particularly restrictive when higher altitude photography is required to give a large enough field of view so as to encompass sufficient reference landmarks. It should be mentioned here that this restriction is more severe for the various environmental satellites because of the limited number of passes of the satellite over the area to be studied in any given time.

Most of these problems, however, are avoided in the present system, due to the increased position accuracy ( $\leq 10$  m) and the ability to work at low altitudes even when large areas need be covered. An additional advantage in the present system is that the mapping data is stored in digital form thus bypassing the digitization phase which is often ultimately required in many of the more conventional monitoring techniques discussed above. This feature is particularly useful in producing scaled plots of the data which may be readily overlaid on available maps of the study area. The results of several test flights of the present system involving various oceanographic measurements are discussed below.

In the first test, a flight was organized in conjunction with ocean dumping experiments carried out by the Pacific Region of Ocean and Aquatic Sciences (OAS) in February 1976. The purpose of the experiments was to ascertain some of the ecological and chemical effects of dumping various material at sea. During each dump various monitoring techniques employing drogues, dyes, bottom samples, etc. were used to study the effective dispersal of the dump material as a function of time. The dump area is located off Point Grey near the City of Vancouver and is the largest dump site in Canada for ocean dumping disposal of waste material. The particular dump which was monitored occurred at 1335 hrs. on February 9 and consisted of coarse Fraser River dredge material. During the monitoring the aircraft was flown at an altitude of 300 m in a roughly circular path encompassing the nominal dump site and reference landmarks at Pt. Atkinson, Cowan Pt. and a marker light off Pt. Grey. The average time interval between landmarks for this circuit was about 2.5 minutes (150 secs). A map showing the calculated position of the sighted dump material and the landmarks is shown in Fig. 4. Here, an enlarged view of the dump material is shown in insert, with the numbers indicating the approximate time to the nearest minute into the dump.

A total of six passes were made over the dump material after dumping commenced. Because of uncertainty in knowing exactly when the dump was to occur (due to lack of communication between the aircraft and the dumping barge) it was necessary for the aircraft to maneuver over the dump area for a considerable length of time before the actual dump. This was not an ideal situation, unfortunately, for determining the INU drift because of the aircraft's accelerations during the maneuvers and because it was not possible during this time to sight a reference landmark. After dumping commenced, however, it was possible to sight the marker light off Pt. Grey between the fourth and fifth pass over the dump material which significantly reduced

interpolation errors in the drift curve. From the drift data, it is estimated that the absolute position error for the dump material during any pass should be less than 15 m. In addition to the sighting data, color photographs were taken of the dump material using a 70 mm Hasselblad camera mounted in the belly of the aircraft.

The results of the mapping test, as shown in Fig. 4 indicate that the visible portion of the dump material had a physical extent of about 600 m and, during the 8 minutes in which the material was monitored, underwent a roughly counter-clockwise rotation with a maximum displacement of about 90 m implying velocities of the order of 0.2 m/s. It should be mentioned, however, that the dump material became very difficult to see during the last two passes and thus some of the movement may well be due to operator sighting inaccuracies. Aside from the above movement, however, no bulk displacement of the dump material is evident. Examination of color photographs taken of the dump material during the first four passes indicates that the material was reasonably visible within one or two minutes after the dump. After this time the visibility decreased noticeably. Unfortunately, due to the limited field of view of the camera at this altitude, it was not possible to correlate the position of the dump material from the photographs with the MIDAS data.

In a second study, the development of a distinct river silt plume front was mapped at the mouth of the Fraser River south of Vancouver. Here again, a roughly circular path was flown, however, on this occasion at an altitude of 900 m. A higher altitude was used in order to provide for an increased field of view of the area to be studied. This did, however, result (as expected) in a slightly larger experimental error. Figure 5 shows a map of the calculated positions of the silt plume front and the reference landmark used overlaid on a chart of the area. Approximately four passes were made along the length of the front over a time period of about 80 minutes, the average time interval between landmarks being approximately 11 minutes (660 secs). During each pass sightings were also taken of the individual light stations along Steveston Jetty. Comparison of the calculated positions for each of the stations with actual positions obtained from a 12,000:1 scale map of the area showed average latitude and longitude errors of  $2.5 \pm 10$  m and  $-2.5 \pm 19$  m respectively. As was mentioned above, the somewhat increased standard deviation is attributed to the higher aircraft altitude. This may be seen by averaging the target position errors for the first pass over the light stations which was carried out at a lower altitude of 300 m. The averages for these taken alone were  $-5 \pm 5$  m and  $10 \pm 6$  m respectively, and are consistent with those obtained in earlier tests.

From the results of the mapping operation (Fig. 5), similar regions of the front can be identified as the plume spreads enabling the velocity of the front in these regions to be approximated from consecutive sightings. These are shown as velocity vectors in Fig. 5. Assuming position errors of  $\leq 20$  m for each sighting, the error in velocity should be  $\leq 0.03$  m/sec. As is seen, the major portion of the front moved in a north to northwest direction at velocities ranging from 0.2 to 0.6 m/sec. This movement is against the tidal flow in the strait which is ebbing ( $\approx 0.25$  m/s SE) and can be attributed to the strong SE wind ( $\approx 14$  m/sec) which existed for the duration of the flight.

Various test flights have also been conducted in order to measure surface water currents by monitoring the movement of floating target drogues. The drogues used in these studies were constructed of four foot square sections of  $\frac{1}{4}$  inch plywood. Each target drogue was painted fluorescent orange in color and was numbered (0 - 9) on one side such that individual targets in a string could be readily identified from the air by the sight operator. The size of the targets provided reasonably good visibility at an aircraft altitude of 300 m, the altitude flown for these tests. During the initial test flights, the targets were laid along a predetermined line in the study area using a motorized launch. This technique, however, provided no flexibility in that the target line could not be altered during flight in order to take advantage of any obvious physical features. To overcome this problem, it was arranged that the launch would lay the targets in response to instructions given in the aircraft. Communication between the launch and the aircraft was provided by CB

radio and proved to be more than adequate for the range of distances involved (< 6 km).

Several of these test flights were carried out in the fall of 1976 in Haro Strait, a body of water approximately 11 km wide between the lower Vancouver Island mainland and the U.S. San Juan Island. During this time OAS (Pacific) and the U.S. National Oceanic and Atmospheric Administration (NOAA) were also conducting a program of ocean current measurements in Haro Strait providing an opportunity for comparison of current measurements.

Two such test flights were carried out on Sept. 9, 1976 involving two separate target strings in each flight. Monitoring of each target string lasted for about 30 minutes with up to six passes being made over each target in the string. Upon completion of the monitoring of each string, the launch retrieved the targets before commencing to lay the next string. The average time interval between consecutive passes over any one target in any string was about 7 minutes which resulted in a calculated velocity accuracy of  $\approx 0.05$  m/sec (assuming 10 m accuracy in each target sight). After each pass, the aircraft would continue on to the nearest reference landmark for a position fix. For this particular study area, four surveyed landmarks were available. A map showing the position of the landmarks and the interpolated positions and velocities of each target, for three of the target strings, are shown in Fig. 6. Also given are the positions of the six NOAA current meter stations in the immediate area. It should be mentioned here, that due to the fact that the airborne monitoring encompassed a total time of about 3 hrs, Fig. 6 cannot be interpreted as a surface current record at any one instant of time. Given the tidal conditions that existed during the monitoring period, it is expected, however, that the general features of the flow remained relatively constant.

Current velocity and direction data from each of the NOAA stations was available at various depths ranging from a minimum of 4 m to a maximum of 183 m. The actual depths available from each station in addition to other relevant data are listed in Table I.

TABLE I. NOAA Current monitoring stations in Haro Strait.

Stn #	Latitude	Longitude	Sensor Depth(s) (m)	Water Depth (m)
62	48:27:50	-123:07:02	4.6, 21.3, 184	199.5
63	48:27:12	-123:09:13	4.6, 21.3	141.5
64	48:26:20	-123:12:21	4, 20.7, 72	87.2
101	48:30:40	-123:10:52	12.2	251.6
104	48:30:30	-123:12:26	12.2, 21.3	193.1
105	48:29:51	-123:16:28	4.6, 21.3, 51.2	66.5

Direct comparison of the airborne and NOAA data was made difficult by the fact that no surface current measurements were available at the NOAA stations. Subsurface currents will, in general, differ from surface currents depending on such factors as depth, stratification of the water column and environmental conditions (particularly wind). During the time of both flights (0930 - 1230 hrs) there was a southerly tide and a relatively strong north wind ( $\approx 5$  m/sec). The affect of this wind on the surface current was to increase the velocity depth gradient resulting in a significant difference between surface and subsurface current measurements. This may be seen by considering the data from target line C in Fig. 6. For these data, the target drogue velocities were averaged together for each pass in order to obtain a mean velocity of the water surface (over the area of the target string) as a function of time. Comparison of these data with data from neighboring NOAA stations, near the surface, are shown in Fig. 7. As is evident, the measured mean surface currents are 0.5 - 1.0 m/sec higher than the corresponding NOAA data. Similar results were obtained from target string A. It is evident, however, that the general nature of the flow as measured from the surface drogues is in substantial agreement with the NOAA data taken as a whole.

In addition to surface current measurements, it was hoped that airborne monitoring of floating target drogues could provide useful data on various flow anomalies such as tide lines or eddies. To study this possibility, target



line B was laid across a visible tide line (solid line in Fig. 6) extending from Discovery Island to San Juan Island. Two passes of the aircraft were made over the tide line in order to map its position and relative velocity. The first pass occurred before monitoring of the target drogues in line B began and the second occurred during the monitoring. The position of the tide line was particularly fortuitous in that its direction of motion carried it past two of the NOAA stations (62 and 63). The current velocity and direction data from stations 62 and 63 (for a depth of 4.6 m) is plotted in Fig. 8 as a function of time. As is evident the current velocity and to a lesser extent, the direction, change noticeably as the tide line passes each station. The vertical lines indicate the predicted time at which the tide line passed each station, obtained from the approximate tide line velocity calculated from the two airborne sightings. These predictions correlate well with the actual times of measured current change. The difference in the measured surface currents, from target string B, on either side of the tide line shows reasonable agreement with the same difference obtained from the NOAA data from station 63. Some deviation should be expected, however, due to the fact that the locations of the two target drogues and NOAA station 63 did not coincide exactly. Examining the various velocities, it is seen that the surface velocity of the tide line is intermediate between that of the flows on either side of the line indicating that debris will be swept into the line from both sides, a result which is consistent with general observations of tide line behavior.

## 6. CONCLUSIONS

A hybrid airborne inertial navigation system comprising a Litton LTN-51 inertial navigation unit and a target sight has been tested for use in aircraft track recovery and airborne mapping of surface targets and/or features. The target sight, which is located in the transparent nose of the aircraft, is used to establish the position drift of the inertial unit at discrete times by fixing the position of the aircraft relative to known surface landmarks. By fitting a modified cubic spline to the discrete drift data, theoretical and experimental tests have shown that the aircraft's track and the position of any additional sighted targets may be determined at any time during the flight to within the RMS error in the individual position fixes provided that these are obtained at least every 10 minutes in time. For the present experimental system, this represents a ground error of about 5 m at an aircraft altitude of 300 m. This error increases for increasing altitudes because of inaccuracies in the target sight and in the barometric altitude indication used. We are currently planning to improve this accuracy with the installation of a precision radar altimeter.

With the accuracies mentioned above, this system is eminently suited for any airborne remote sensing application requiring accurate position information. In the area of coastal oceanography this system has particular application in that the target sight may also be used to monitor the movement of the surface water in a variety of situations. The increased accuracy and flexibility of operation provide real advantages over more conventional oceanographic monitoring techniques such as aerial photography or radar/VLF positioning, and the digital recording simplifies data analysis.

## 7. REFERENCES

1. G.E. Beck , Ed. Navigation Systems, Van Nostrand Reinhold, London 1971.
2. C. Sangiovanni and J. Moryl, Mixed Inertial Navigation Systems, Navigation 21, 61 (1974).
3. R.L. Grasty, J.F.R. Gower and B.M. Oliver, Inertial Navigation for Flight Path Recovery, Proc. Geological Survey of Canada, 1977.
4. R.C. Baker and J.S. MacDonald, An Integrated Airborne Data Acquisition System for Remote Sensing, 2nd Can. Rem. Sens. Symp., Guelph, Ontario, Canada, 1974.
5. D.B. Reid and R.K. Harman, Optimal Filtering and Smoothing of Navigation Sensor Data for Resource Exploration and Development, Can. Aeronautics and Space J. 21, 41 (1975).

6. R.E. Kalman, A New Approach to Linear Filtering on Prediction Problems, Trans. ASME, Ser. D: Journal of Basic Engineering, 83, 1961.
7. R.C. Garvine, Physical Features of the Connecticut River Outflow During High Discharge, J. Geophys. Res. 79, 831 (1974).
8. V. Klemas, M.W. Leathan, P. Kinner, and W. Treasure, Dye and Drogue Studies of Spoil Disposal and Oil Dispersion, J. WPCF 46, 2026 (1974).
9. A.E.P. Watson, Ed. Workshop on the Feasibility of Remote Tracking of Drogues, Proc. of Int. Joint Comm., Windsor, Ont. Canada, Feb. 24-25, 1975.

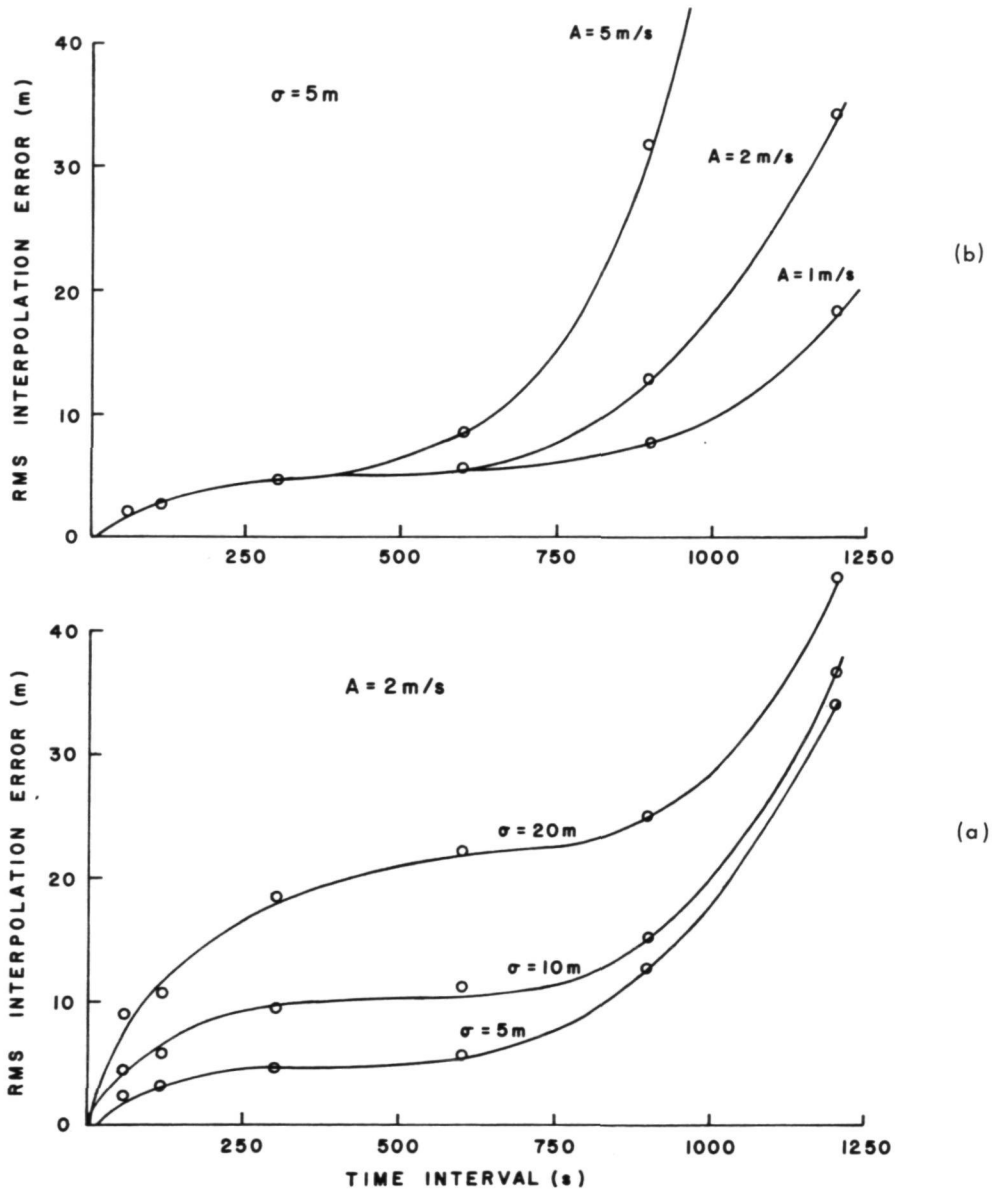


FIGURE 1. ERROR IN FITTING A CUBIC SPLINE TO DISCRETE DATA GENERATED ASSUMING A SINUSOIDAL INERTIAL SYSTEM DRIFT.

6071

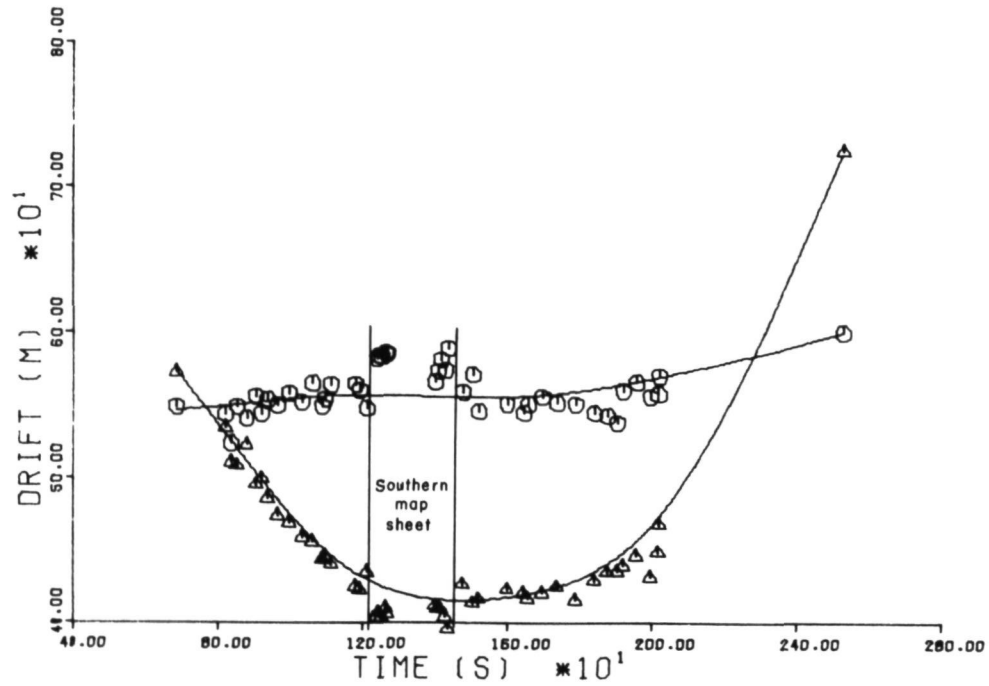


FIGURE 2. INERTIAL SYSTEM DRIFT DURING THE PATRICIA BAY HIGHWAY TEST FLIGHT. The data represents the error in position for major road intersections along the highway. The upper curve is the latitude drift and the lower the longitude drift.

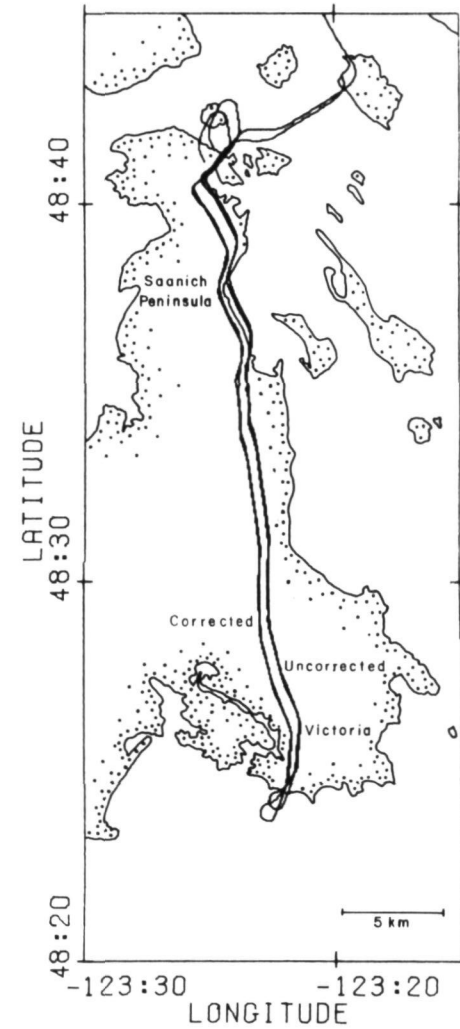


FIGURE 3. MAP OF THE CORRECTED AND UNCORRECTED FLIGHT PATHS FOR THE PATRICIA BAY HIGHWAY TEST FLIGHT.

ORIGINAL PAGE IS  
OF POOR QUALITY

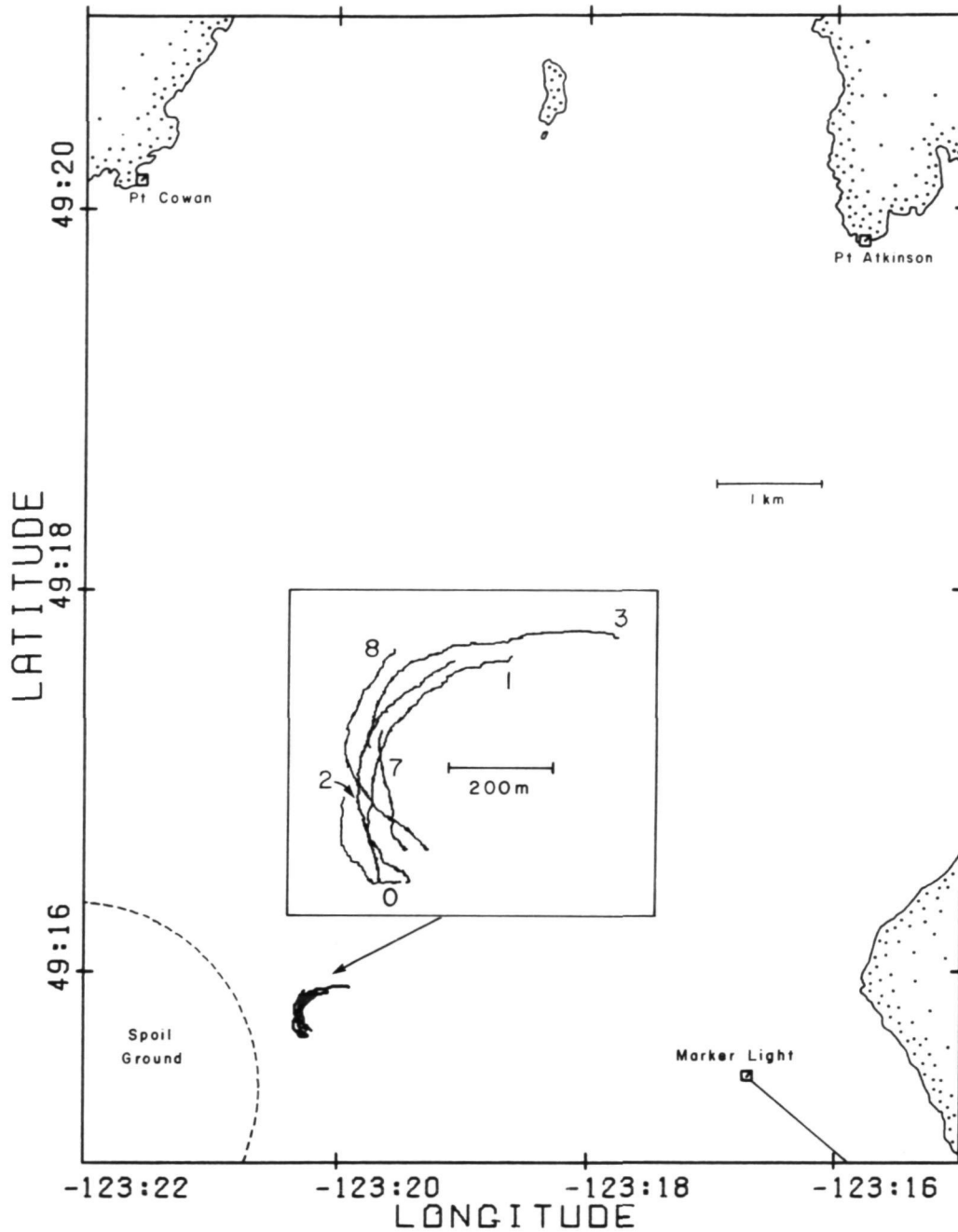


FIGURE 4. MAP OF DUMP MATERIAL FOR THE OCEAN DUMP EXPERIMENT MONITORED ON FEB. 9, 1976. The insert shows an expanded view of the dump material showing the sequential positions for each aircraft pass. The numbers indicate the time of each pass in minutes into the dump.

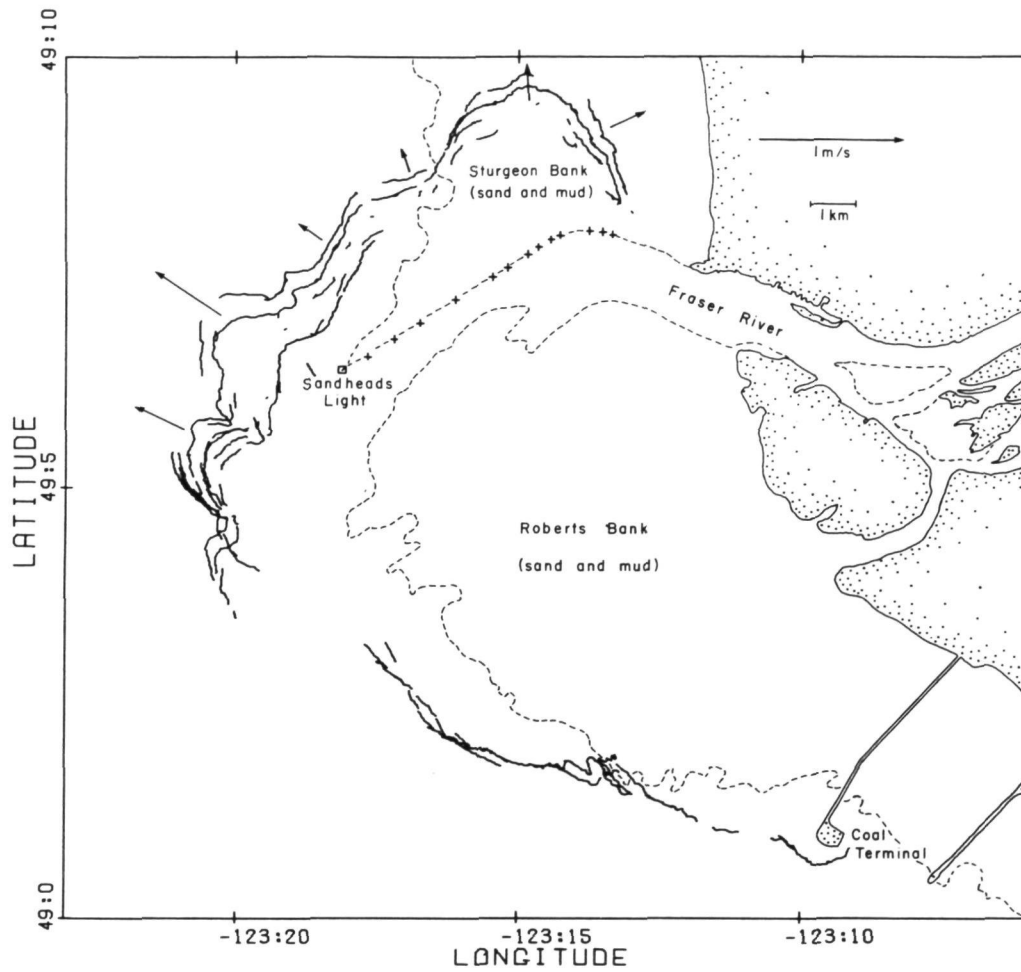


FIGURE 5. MAP SHOWING SEQUENTIAL POSITIONS OF THE SILT PLUME FRONT OFF THE MOUTH OF THE FRASER RIVER NEAR VANCOUVER, B.C. Estimates of the front velocity obtained from the time of each pass are shown as velocity vectors. Also shown are Sandheads light (the reference landmark) and the light stations along Steveston Jetty.

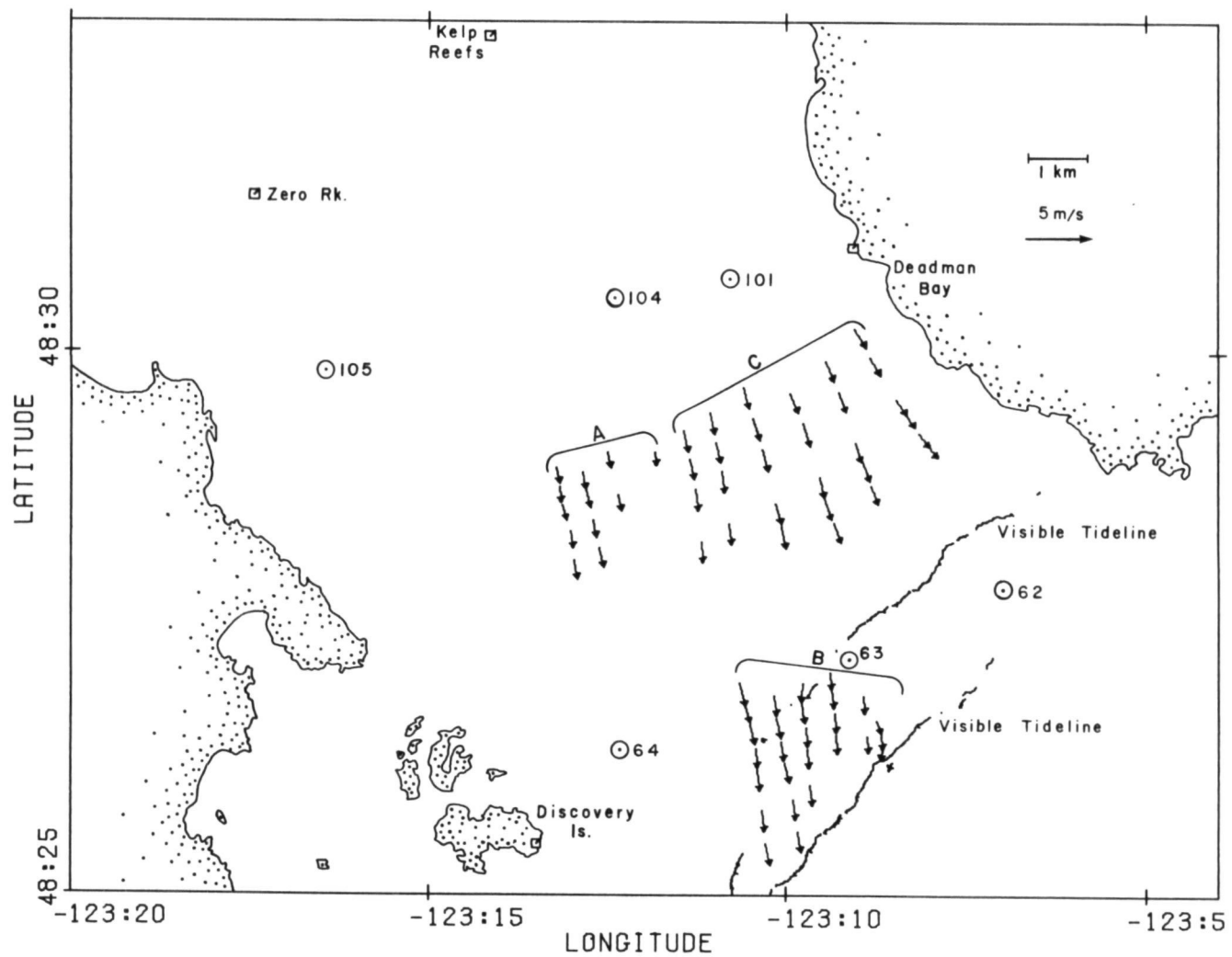


FIGURE 6. DROGUE VELOCITIES IN HARO STRAIT BETWEEN 0930 AND 1230 ON SEPT. 9, 1976. The numbered circles indicate the positions of the six NOAA current meter stations in the study area.

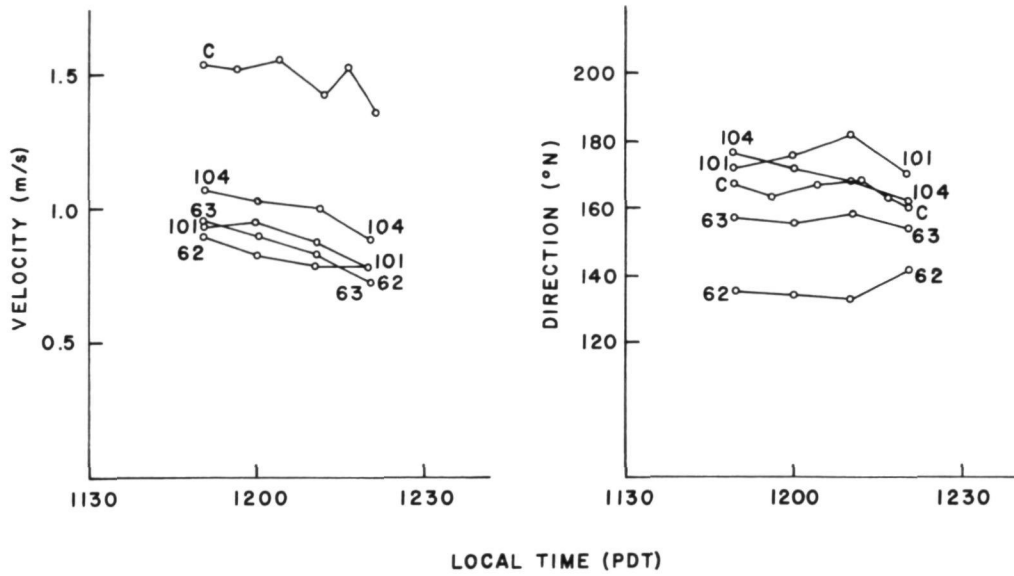


FIGURE 7. COMPARISON OF DROGUE AND NEAR SURFACE NOAA CURRENT DATA. The drogue data is from string C (Figure 6).

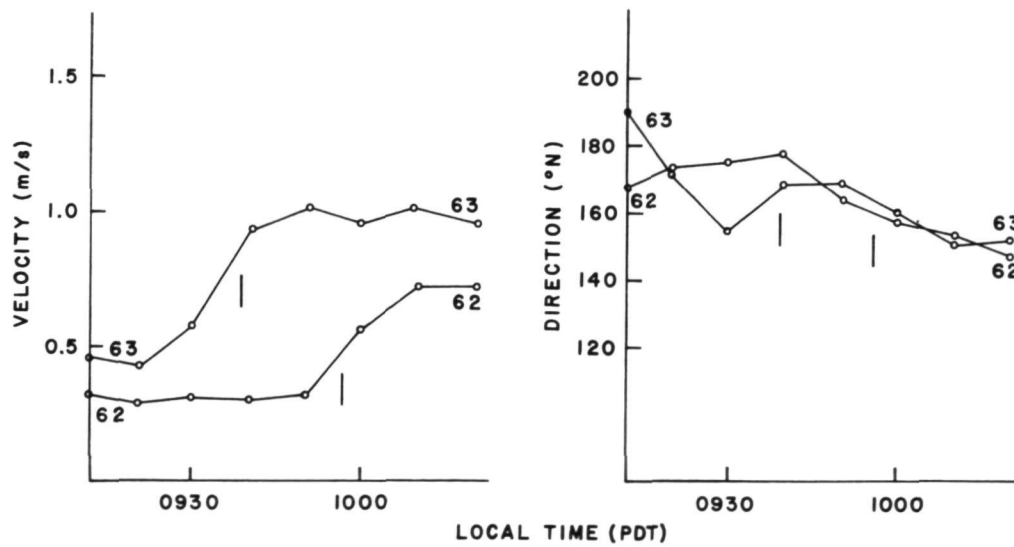


FIGURE 8. NEAR SURFACE CURRENT DATA FROM NOAA STATIONS 62 AND 63. The solid vertical lines indicate the predicted time of crossing of the tide line obtained from the observed tide line velocity.